



Recoverable visible light photocatalytic activity of wide band gap nanotubular titanic acid induced by H₂O₂-pretreatment



Yan Wang^{a,b}, Xiangjiang Meng^a, Xinluan Yu^a, Min Zhang^a, Jianjun Yang^{a,*}

^a Key Laboratory for Special Functional Materials of Ministry of Education, Henan University, Kaifeng 475004, PR China

^b Basic Experiments Teaching Center, Henan University, Kaifeng 475004, PR China

ARTICLE INFO

Article history:

Received 21 January 2013

Received in revised form 21 February 2013

Accepted 1 March 2013

Available online 14 March 2013

Keywords:

Nanotubular titanic acid

H₂O₂-pretreatment

Photocatalyst

Ti-peroxide complexes

Propylene oxidation

ABSTRACT

Nanotubular titanic acid (denoted as NTA) with orthorhombic crystal structure was prepared by combining hydrothermal treatment of TiO₂ in alkaline medium with follow-up pickling. Resultant NTA was further treated with the aqueous solution of H₂O₂ to extend its light absorbance responses to visible light region thereby acquiring visible light photocatalytic activity. The photocatalytic performance of as-prepared NTA modified by H₂O₂ (denoted as H₂O₂-NTA) was evaluated by monitoring the oxidation of propylene under visible light irradiation. Moreover, as-fabricated H₂O₂-NTA was annealed at 300 °C in air to examine its thermal stability, and used H₂O₂-NTA was retreated with aqueous H₂O₂ at the end of the third run of propylene oxidation tests to allow regeneration. Results indicate that pretreatment with aqueous H₂O₂ provides NTA with apparent visible light photocatalytic activity for the oxidation of propylene. H₂O₂-pretreatment results in a large amount of Ti-peroxide complexes on the surface of NTA; resultant Ti-peroxide complexes serve as visible light absorbing sensitizers and are excited by visible light in association with the state change from the ground state to the excited state. As a result, an electron is injected from the excited state of Ti-peroxide complexes to the conduction band of NTA, thereby generating O₂^{•-} radical possessing strong oxidation ability to initiate the degradation of propylene. The visible light photocatalytic activity of H₂O₂-NTA gradually declines with extending photocatalytic reaction time, which is attributed to the gradual consumption of active Ti-peroxide complexes therewith. However, the lost visible light photocatalytic activity of H₂O₂-NTA can be regenerated by retreatment with aqueous H₂O₂. In this way, the visible-light-responses and photocatalytic activities of NTA, an orthorhombic crystalline rather than anatase or rutile phase TiO₂, is well regenerated.

© 2013 Elsevier B.V. All rights reserved.

1. Introduction

In 1998–1999, Kasuga et al. reported a novel nanotubular material prepared via alkali hydrothermal method and regarded it as nanotubular TiO₂ [1,2]. Since then, such a so-called nanotubular TiO₂ has been extensively investigated, since its large surface area and mesoporous structure provide prerequisites for it to be used as a promising photocatalyst [3]. Zhang et al. also obtained the so-called nanotubular TiO₂ by making use of the method reported by Kasuga [4]. However, Du et al. suggested that the so-called nanotubular TiO₂ reported by Kasuga et al. and Zhang et al. should be actually nanotubular TiO_x or H₂Ti₃O₇ [5,6]. Yang et al., after determining the content of Na, Ti and structural water of the so-called nanotubular TiO₂, claimed that it is actually nanotubular sodium titanate (molecular formula: Na₂Ti₂O₄(OH)₂) which can be converted to nanotubular titanic acid (molecular formula:

H₂Ti₂O₄(OH)₂) by ion exchange with hydrochloric acid solution of pH 1 [7]. From then on, the morphology, crystal structure, optical properties, and photocatalytic performance of NTA and its derivatives have been extensively and meticulously studied [8–13].

The band gap of NTA is in the range of 3.38–3.87 eV [14,15], higher than the intrinsic band gap of powder TiO₂ (anatase: 3.2 eV; rutile: 3.0 eV), which means that NTA is generally insensitive to visible light and it is of significance to fabricate visible light active NTA. Fortunately, NTA could be endowed with visible light activity by doping with metal or non-metal elements, decorating with quantum dot, and coupling with semiconductor. For example, Jiang et al. obtained visible-light-responsive tubular N-doped anatase nanotubes by solvothermally treating NTA suspension with NH₄Cl in ethanol–water at 120 °C [16]; and they proposed that NH₃ is adsorbed on the walls of titanic acid nanotubes to form ammonia titanate which is then transformed to visible-light-responsive N-NTA upon annealing. Ratanatawanate et al. prepared PbS and CuS quantum dots and decorated them, respectively, on both the inside and outside surfaces of NTA by using different linkers [17,18]. As-obtained PbS or CuS quantum dot/NTA composites show

* Corresponding author. Tel.: +86 378 3881358; fax: +86 378 3881358.

E-mail addresses: desertsea8079@yahoo.cn (Y. Wang),

yangjianjun@henu.edu.cn (J. Yang).

apparent visible light catalytic activities for the photodegradation of organic dyes and photodecomposition of malachite green and phenol. Recently, Zhai et al. fabricated graphene hybridized NTA nanocomposites by hydrothermal method. They found that as-prepared graphene hybridized NTA nanocomposites possess large BET surface area and outstanding photocatalytic activities for the decomposition of Rhodamine-B under visible light illumination [19], which is suggested to be attributed to visible light sensitization by graphene rather than by the impurity level in the band gap of NTA.

Viewing the aforementioned literature survey and noticing that no report is currently available about the preparation of visible-light-active NTA with the assistance of pretreatment in aqueous H_2O_2 , in the present research we adopt a simple impregnating method to fabricate H_2O_2 modified NTA at room temperature. In the meantime, the photocatalytic behavior of NTA, P25 (Degussa product) and as-prepared H_2O_2 -decorated NTA for the photocatalytic oxidation of propylene under visible light irradiation was evaluated. This article reports the fabrication as well as structural characterization and photocatalytic performance evaluation of H_2O_2 -decorated NTA photocatalyst.

2. Experimental

2.1. Preparation of H_2O_2 -decorated NTA photocatalyst

H_2O_2 -decorated NTA (denoted as H_2O_2 -NTA) photocatalyst was prepared by a two-step route. Briefly, a proper amount of commercially obtained P25 powder was added into the aqueous solution of NaOH (10 mol L^{-1}) and magnetically stirred to allow uniform mixing. Resultant mixed solution was autoclaved at 120°C for 48 h, followed by naturally cooling to room temperature to afford precipitate. As-obtained precipitate was washed repeatedly with de-ionized water to a pH of ca. 7.0–8.0 and immersed in the aqueous solution of HCl (0.1 mol L^{-1}) overnight under magnetic stirring. Upon completion of immersion in HCl solution, the precipitate was washed again with de-ionized water to remove Cl^- and dried at room temperature under vacuum, yielding NTA. Then about 1.4 g of as-obtained NTA was immersed into 20 mL of aqueous solution of H_2O_2 (mass fraction 2 wt.%) and magnetically stirred for 1 h, followed by filtration to afford precipitate. Resultant precipitate was dried at room temperature under vacuum to afford visible-light-active NTA denoted as H_2O_2 -NTA. H_2O_2 -P25 as a reference was prepared in the same manners. Moreover, as-prepared H_2O_2 -NTA was annealed at 300°C in air for 2 h to investigate its thermal stability, and relevant annealed sample is denoted as H_2O_2 -NTA-300 (here suffix 300 refers to temperature at which as-fabricated H_2O_2 -NTA is annealed).

2.2. Characterization of H_2O_2 -decorated NTA photocatalyst

The morphologies of various photocatalyst samples were observed with a JEM-2010 transmission electron microscope (TEM). X-ray diffraction (XRD) patterns were measured with an X'Pert Philips diffractometer (Cu K α radiation, 2θ range 10 – 90° , step size 0.02° , accelerating voltage 40 kV , applied current 40 mA). Ultraviolet-visible light (abridged as UV-vis) absorption spectra were recorded with a Hitachi U-4100 UV-vis near infrared spectrophotometer (reference: $BaSO_4$). A Kratos AXIS Ultra X-ray photoelectron spectroscope (XPS) was performed to analyze the chemical states of major elements in various photocatalysts (excitation source: monochromatized Al K α radiation ($h\nu = 1486.6\text{ eV}$); power 150 W ; 15 kV and 10 mA). XPS data were collected at an analysis chamber pressure of below 10^{-8} – 10^{-9} torr while the binding energy of hydrocarbon (C 1s: 284.8 eV) was used as an internal

standard for the correction of charging shift. The survey spectra and core level spectra were collected at pass energies of 80 eV and 40 eV , respectively.

In addition, terephthalic acid (denoted as TA) was used as a probe to monitor the change of hydroxyl radical content of H_2O_2 -NTA suspensions before and after visible light irradiation, since TA can readily react with $^{\bullet}\text{OH}$ radical to generate TAOH which emits fluorescence around 426 nm under the excitation of its own absorption band at 312 nm . Briefly, about 90 mg of as-fabricated H_2O_2 -NTA was dispersed in 30 mL of mixed aqueous solution of NaOH (20 mmol L^{-1}) and TA (6 mmol L^{-1}). Resultant mixture was divided into two equant parts: one was kept in dark, and another was irradiated by visible light ($\lambda \geq 420\text{ nm}$). The two equant parts were separately magnetically stirred for 1 h and then centrifuged to afford the liquid for photoluminescence (abridged as PL) measurement with a Gilden FluoroSENS fluorescence spectrometer. The content of $^{\bullet}\text{OH}$ radical in H_2O_2 -NTA suspensions before and after visible light irradiation was compared based on PL data.

2.3. Evaluation of visible light photocatalytic activity

The photocatalytic activity of P25, NTA, H_2O_2 -P25, H_2O_2 -NTA and H_2O_2 -NTA-300 was evaluated by monitoring the oxidation of gaseous propylene under visible light irradiation. Briefly, about 30 – 35 mg of each sample was separately suspended in an appropriate amount of distilled water. A few drops of resultant suspension were spread on one side of a roughened glass plate (working surface, area: about 10 cm^2) and dried at 70°C in air. Then the coated glass plate was placed in a flat quartz tube reactor equipped with a 500 W xenon lamp as the visible light source. Between the xenon lamp and reactor were inserted a cut filter ($\lambda \geq 420\text{ nm}$) and a water cell to eliminate ultraviolet and infrared light, respectively. The intensity of the light irradiated on to-be-tested samples with $\lambda \geq 420\text{ nm}$ is about 20 mW/cm^2 . Feed gas consists of C_3H_6 and air stored in a high-pressure cylinder. The flow rate of the feed gas was adjusted to ca. 150 mL h^{-1} ; and the concentration of C_3H_6 was determined with a chromatograph (Shimadzu GC-9A) equipped with a flame ionization detector and a GDX-502 column. The removal rate of C_3H_6 was calculated as $(C_0 - C)/C_0 \times 100\%$, where C_0 refers to the initial concentration of C_3H_6 (600 ppm V) and C refers to the concentration of C_3H_6 measured upon the completion of its photocatalyzed oxidation. Moreover, photocatalyzed oxidation tests of propylene were also conducted to examine the stability, repeatability, and regeneration of sample H_2O_2 -NTA. For this purpose, photocatalyst sample H_2O_2 -NTA coated on the glass slide was placed in the flat quartz tube reactor to undergo a total of three runs of propylene oxidation tests in sequence. The photocatalytic activity at the end of each run was measured. At the same time, upon completion of the third run, a few drops of fresh aqueous H_2O_2 (2 wt.%) was dropped onto the working surface of the coated glass slide and dried at 70°C in air to allow regeneration; and then the visible light photocatalytic activity of the resurrected-sample (i.e., the regenerated activity of sample H_2O_2 -NTA) was directly evaluated without drying in vacuum.

3. Results and discussion

3.1. TEM morphology analysis

It is well known that P25 samples are consist of nanoparticles with a diameter of 20 – 30 nm , which is well in accordance with the results shown in Fig. 1(b). As can be seen from Fig. 1(a), NTA has a layered structure, with the distance between the adjacent layers being about 0.8 nm , in agreement with our previous

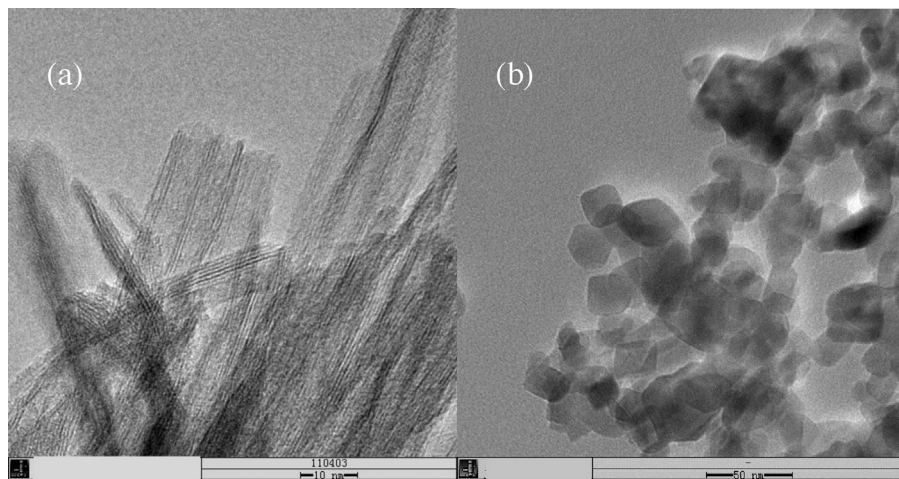


Fig. 1. TEM pictures of samples (a): NTA and (b): P25.

researches and other reports [1–9]. The layered structure is considered to be beneficial to form more Ti–OH species because it contains both intralayered and interlayered OH groups [8]. After H_2O_2 -pretreatment, the morphology of NTA and P25 is not changed and then the TEM pictures are not given here.

3.2. XRD analysis

Fig. 2 shows the XRD patterns of NTA, H_2O_2 -NTA, H_2O_2 -NTA-300, P25, and H_2O_2 -P25. NTA belongs to orthorhombic system and shows characteristic diffraction peak around $2\theta = 9^\circ$, which is well elucidated elsewhere [8]. After H_2O_2 -pretreatment, resultant H_2O_2 -NTA sample retains the orthorhombic crystalline structure of NTA, which demonstrates that H_2O_2 -pretreatment does not change the crystalline form of NTA. Besides, sample H_2O_2 -NTA-300 obtained after annealing H_2O_2 -NTA at $300^\circ C$ in air for 2 h still maintains the orthorhombic crystalline form, which well corresponds to our previous finding that orthorhombic NTA is transformed to anatase TiO_2 phase around $400^\circ C$ [8,11,12,20–22]. Moreover, similar to the cases for samples H_2O_2 -NTA and H_2O_2 -NTA-300, pretreatment in the aqueous solution of H_2O_2 does not cause changes in the crystal structure of P25 (containing anatase TiO_2 as the major phase and rutile TiO_2 as the minor phase) either (see Fig. 2(d) and (e)).

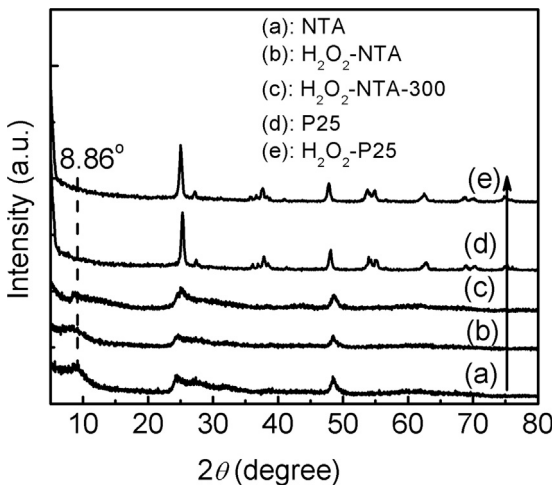


Fig. 2. XRD patterns of samples NTA, H_2O_2 -NTA, H_2O_2 -NTA-300, P25, and H_2O_2 -P25.

3.3. Optical absorption properties of various photocatalysts

The optical absorption spectra of NTA, P25, H_2O_2 -P25, H_2O_2 -NTA, and H_2O_2 -NTA-300 are comparatively shown in Fig. 3. Both NTA and P25, with white color, do not show any visible light absorption, since they have a wide band gap (NTA even possesses a larger band gap than P25 as can be derived from the bandedge absorption from Fig. 3A). H_2O_2 -P25 shows a slightly enhanced visible light absorption as compared with P25 (see Fig. 3B). Such a tiny light absorbance enhancement corresponds to almost unchanged color of P25 after pretreatment in aqueous H_2O_2 . However, sample H_2O_2 -NTA shows significantly enhanced visible light absorption in the range of 400–500 nm as compared with pristine NTA and P25. This may be closely related to the substitution of the –OH group on TiO_2 surface by the –OOH group of H_2O_2 resulting in yellow titanium peroxide complexes [23–30], as evidenced by the vivid yellow color of sample H_2O_2 -NTA. Namely, more –OH group is present on the surface of NTA rather than TiO_2 [8], which facilitates the formation of more Ti-peroxide complexes on the surface of NTA but not P25. As-formed Ti-peroxide complexes are capable of absorbing visible light; and the more the Ti-peroxide complexes adsorbed on the surface are, the better the visible light absorption capacity is [24]. This is why sample H_2O_2 -NTA shows considerably improved optical absorption behavior. To further validate that Ti-peroxide complexes function as visible light absorbing sensitizers, we annealed sample H_2O_2 -NTA at $300^\circ C$ in air and evaluated the visible light absorbing capacity of resultant sample H_2O_2 -NTA-300 (see Fig. 3A). Unsurprisingly, the visible light absorption capacity of sample H_2O_2 -NTA-300 is much lower than that of sample H_2O_2 -NTA, and it is almost the same as that of P25. This implies that annealing H_2O_2 -NTA at $300^\circ C$ removes most of the pre-adsorbed species including peroxy group, which further proves that Ti-peroxide complexes do function as visible light absorbing sensitizers. Otherwise, sample H_2O_2 -NTA-300 should retain the same visible light absorbing capacity as sample H_2O_2 -NTA. This supposition is also confirmed by visual observation that sample H_2O_2 -NTA-300 does not retain the original vivid yellow color of sample H_2O_2 -NTA but looks almost the same as untreated NTA.

3.4. XPS analysis

Ti 2p spectra of samples NTA, H_2O_2 -NTA, P25 and H_2O_2 -P25 were measured to ascertain the formation of surface Ti-peroxide complexes. As shown in Fig. 4, sample NTA shows spin-orbit components (Ti 2p_{3/2} and Ti 2p_{1/2}) of Ti 2p peak at binding

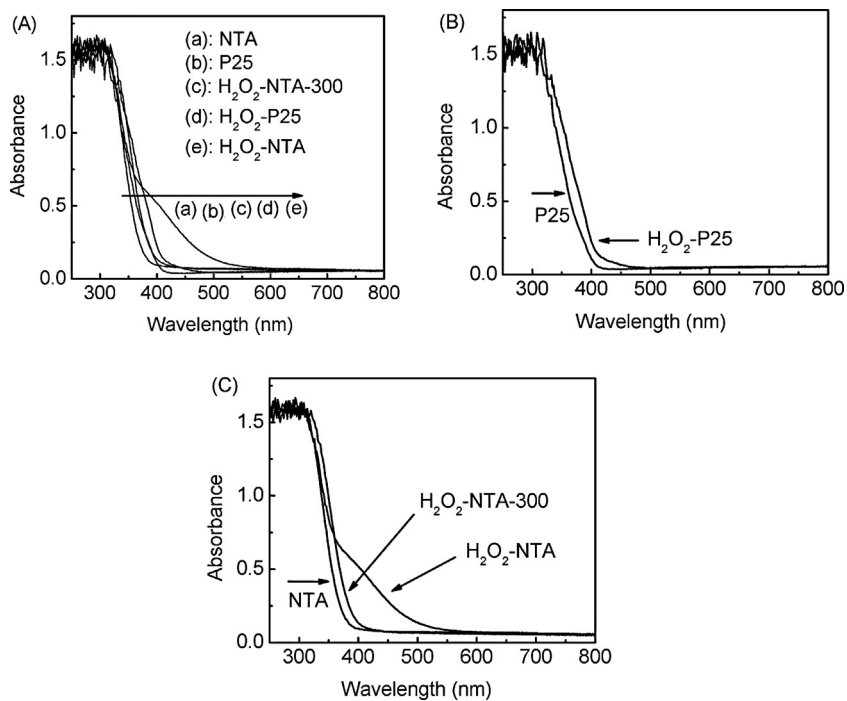


Fig. 3. UV-vis absorption spectra of samples P25, NTA, H_2O_2 -P25, H_2O_2 -NTA and H_2O_2 -NTA-300.

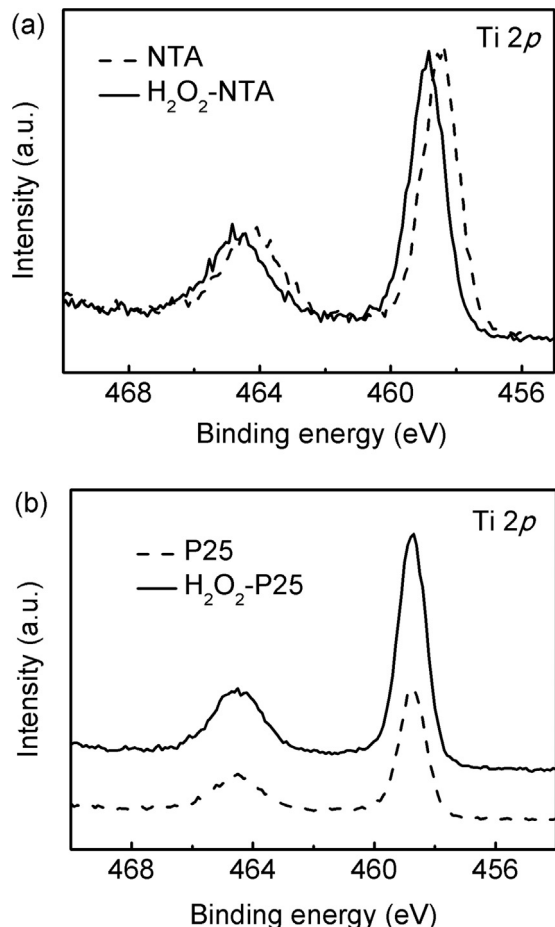


Fig. 4. The change of Ti 2p binding energy between (a): NTA and H_2O_2 -NTA and (b) P25 and H_2O_2 -P25.

energies of 458.4–464.1 eV, which confirms the existence of Ti^{4+} ion (Fig. 4a). Besides, the Ti 2p binding energies of sample H_2O_2 -NTA (458.9–464.6 eV) are shifted toward higher binding energy by about 0.5 eV as compared with that of NTA, possibly due to the formation of Ti-peroxide complexes. This could be rationally understood, since $-\text{OOH}$ group possesses much higher electron withdrawing ability than $-\text{OH}$ group thereby resulting in partial electron transfer from Ti atom to O atom. However, the Ti 2p binding energy of P25 remains unchanged after pretreatment by aqueous H_2O_2 (see Fig. 4b). Considering the abovementioned XPS analytical results, we can infer that H_2O_2 -pretreatment results in different amount of Ti-peroxide complexes on the surfaces of P25 and NTA. It is just the formation of a sufficient amount of Ti-peroxide complexes on the surface of H_2O_2 -NTA that accounts for its much better visible light absorption capacity than P25, H_2O_2 -P25, and NTA.

3.5. Visible light photocatalytic activity

The photocatalytic oxidation removal rate of propylene over photocatalysts NTA, P25, H_2O_2 -P25, H_2O_2 -NTA, and H_2O_2 -NTA-300 under visible light irradiation as a function of reaction time is comparatively shown in Fig. 5. On the one hand, P25 shows a slight photocatalytic activity for the oxidation of propylene and registers a propylene oxidation removal rate of about 5%, possibly because a small amount of ultraviolet light is remained in the light source. On the other hand, sample H_2O_2 -P25 has a slightly higher photocatalytic activity than P25, which demonstrates that H_2O_2 -pretreatment has almost no contribution in enhancing the visible light photocatalytic activity of P25. Differing from P25 and H_2O_2 -P25, sample H_2O_2 -NTA displays greatly enhanced visible light photocatalytic activity for the degradation of propylene, showing a propylene oxidation removal rate of about 21%. As mentioned earlier, the different visible light photocatalytic activities of sample H_2O_2 -NTA in relation to sample H_2O_2 -P25 must be related to its different amount of surface Ti-peroxide complexes. This can be directly proven by dramatically decreased visible light photocatalytic activity of sample H_2O_2 -NTA-300 (its photocatalytic activity is reduced to the level which is almost the same as that

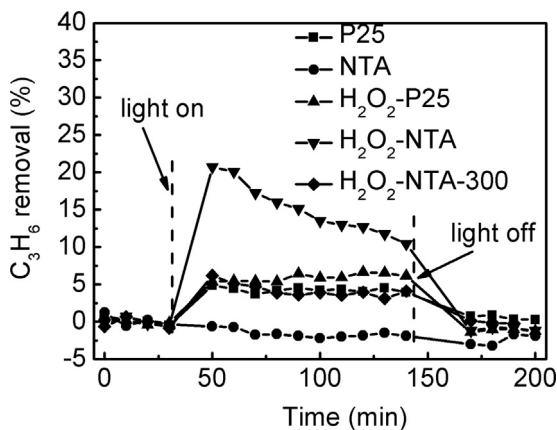


Fig. 5. Photocatalytic oxidation removal rate of propylene over NTA, P25, H_2O_2 -P25, H_2O_2 -NTA and H_2O_2 -NTA-300 under visible light irradiation as a function of reaction time.

of P25, due to removal of Ti-peroxide complexes upon annealing H_2O_2 -NTA at 300 °C in air). Moreover, the visible light photocatalytic activity of H_2O_2 -NTA gradually declines from about 21% to 10% as the reaction time rises from 50 min to about 140 min. This implies that Ti-peroxide complexes are gradually consumed in the photocatalytic oxidation process of propylene. In one word, the different visible light photocatalytic performances of samples H_2O_2 -NTA and H_2O_2 -P25 well correspond to our previous finding that NTA is one of the most promising visible light active photocatalysts [31].

3.6. Stability, repeatability, and regeneration of sample H_2O_2 -NTA

The stability, repeatability, and regeneration of sample H_2O_2 -NTA are shown in Fig. 6. The visible light photocatalytic activity of sample H_2O_2 -NTA tends to gradually decline from the first run to the third run, which is due to the gradual consumption of Ti-peroxide complexes in each run of photocatalyzed oxidation of propylene. To our delight, after sample H_2O_2 -NTA is retreated with aqueous H_2O_2 upon the completion of the third run, it shows very good regenerated visible light photocatalytic activity which is even better than that in the first run. This is possibly because more Ti-peroxide complexes are formed on the surface of H_2O_2 -NTA

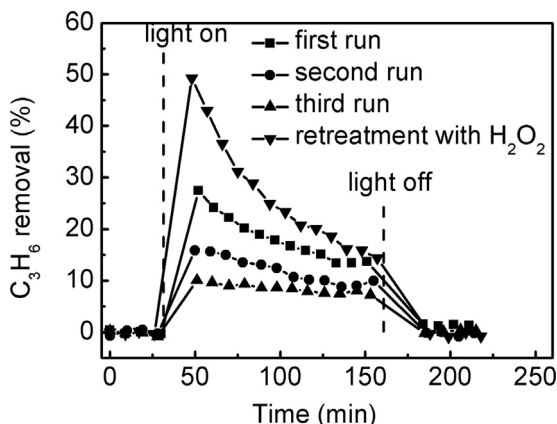


Fig. 6. The stability, repeatability, and regeneration of sample H_2O_2 -NTA for photocatalytic degradation of propylene under visible light irradiation (at the end of the third run, a few drops of 2 wt.% H_2O_2 solution was coated onto the surface of used sample H_2O_2 -NTA and dried at 70 °C in air to allow regeneration).

after it is retreated with aqueous H_2O_2 and not dried in vacuum. In other words, Ti-peroxide complexes can be easily regenerated by retreatment of NTA with aqueous H_2O_2 thereby resulting in drastically recovered visible light photocatalytic activity.

3.7. Visible light photocatalytic degradation mechanism of propylene over photocatalyst H_2O_2 -NTA

Early in 1975, Boonstra and Mutsaers researched the reflection spectra of H_2O_2 -treated TiO_2 powder samples and proposed that the formation of $\cdot H$ radical accounts for photoactivity of TiO_2 under UV illumination [24]. Recently, Li et al. reported that small organic compounds like salicylic acid could be photocatalytically degraded by H_2O_2 -treated P25- TiO_2 under visible light, because of the formation of $\cdot OH$ radical in association with the decomposition of H_2O_2 under visible light irradiation [25]. In terms of the reaction mechanisms, H_2O_2 molecule is adsorbed on TiO_2 surface to form surface Ti-peroxide complexes which extend photo-response to visible light region and are excited by visible light; and an electron is injected from the excited Ti-peroxide complexes to the conduction band of TiO_2 thereby reacting with H_2O_2 adsorbed on TiO_2 surface to generate active $\cdot OH$ radical. Rao and Chu also acknowledge this viewpoint and they suggest that $\cdot OH$ radical plays a dominant role in linuron degradation in Vis/ TiO_2 / H_2O_2 system [28]. Ohno found that rutile shows high visible light photocatalytic activity for the photocatalyzed epoxidation of 1-decene in the presence of H_2O_2 [26]; and they attributed the epoxidation mechanism of olefin to the generation of surface $Ti-\eta^2$ -peroxide complex (under visible light irradiation, one of the oxygen atoms in the peroxy group is transferred to the olefin via a transition state rather than via the generation of electron–hole pairs). Hirakawa et al., combining luminol chemiluminescence probing with terephthalic acid fluorescence probing techniques, suggested that hydrogen peroxide can promote the formation of active oxygen species such as $O_2^{\bullet-}$ and $\cdot OH$ radicals which generally contribute to the photocatalytic reactions [32,33]. All the abovementioned researches point to a common conclusion: the visible light photocatalytic activity of the aqueous TiO_2 suspension in the presence of H_2O_2 is originated from the generation of $\cdot OH$ radical.

Considering the abovementioned research results about the photocatalytic mechanisms of aqueous TiO_2 suspension in the presence of H_2O_2 , we suppose that the prominent photocatalytic activity of sample H_2O_2 -NTA for the oxidation of propylene under visible light irradiation can be described in similar manners. Therefore, it is expected that $\cdot OH$ radicals can also be generated in aqueous H_2O_2 -NTA suspensions under visible light illumination and the results shown in Fig. 7 proves the speculation. One could see that a large amounts of $\cdot OH$ radicals is detected when aqueous H_2O_2 -NTA suspensions was illuminated under visible light with a wavelength of $\lambda > 420$ nm. It can be referred that aqueous H_2O_2 -NTA suspensions have the same behaviors as aqueous TiO_2 suspensions in the presence of H_2O_2 under visible light illumination. Namely, although visible light cannot excite NTA (a kind of wide band gap semiconductor with a forbidden band gap of 3.30–3.87 eV (higher than that of TiO_2 powders)) to generate electron–hole pairs NTA [14,15], treating NTA with aqueous H_2O_2 generates $\cdot OH$ radical under visible light ($\lambda > 420$ nm) illumination thereby inducing visible light photocatalytic activity (see Fig. 7). In other words, the suspension of NTA in aqueous H_2O_2 should have the same visible light photocatalytic behavior as the aqueous suspension of TiO_2 powder in the presence of H_2O_2 . However, our evaluation system is not an aqueous suspension system but a propylene gas one, which means that there is no continuous H_2O_2 molecules adsorbed on the surface of sample H_2O_2 -NTA to react with the conduction band electron of NTA to generate $\cdot OH$ radicals. Considering this point, we suppose that the photocatalytic degradation mechanism of gas propylene

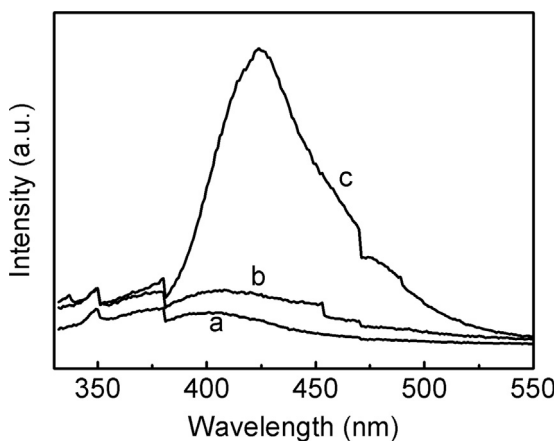
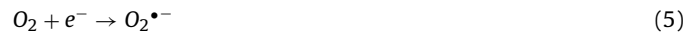
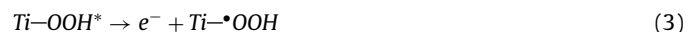


Fig. 7. PL spectra of hydroxyl radicals for TA as reference (a), H_2O_2 -NTA suspension containing TA before visible light irradiation (b), and H_2O_2 -NTA suspension containing TA after visible light irradiation (c).

under visible light irradiation over H_2O_2 -NTA photocatalyst can be described in **Scheme 1**, which is slightly different from those reported elsewhere [24,25,30]. Relevant visible light photocatalytic degradation procedures of gas propylene catalyzed by H_2O_2 -NTA can be depicted by Eqs. (1–6). At the beginning, Ti-peroxide complexes are formed on the surface of NTA upon treatment with H_2O_2 (see Eq. (1)) to shift the photo-response from UV to visible light region, as confirmed in Fig. 3. Resultant surface Ti-peroxide complexes serve as visible light absorbing sensitizers and are excited by visible light in association with the state change from ground state to excited state (see Eq. (2)). In the meantime, NTA functions as an electron acceptor to accept an electron which is injected from the excited state of Ti-peroxide complexes at its conduction band thereby generating $\text{Ti}^{\bullet}\text{OOH}$ radical (see Eq. (3)). Resultant $\text{Ti}^{\bullet}\text{OOH}$ radical is highly active and tends to self-react to resume the original $\text{Ti}^{\bullet}\text{OH}$ species in association with releasing O_2 (see Eq. (4)). Released O_2 captures a conduction band electron to generate $\text{O}_2^{\bullet-}$ radical possessing strong oxidation ability thereby initiating the degradation of propylene (see Eq. (5)). It can be clearly seen from Eqs. (1–5) that the concentration of Ti-OOH complexes is gradually consumed with extending reaction time, which accounts for the loss of the photocatalytic activity of sample H_2O_2 -NTA therewith (see Figs. 5 and 6). However, the lost visible light photocatalytic activity of used sample H_2O_2 -NTA can be regenerated by

retreatment with H_2O_2 (see Eq. (6)). In this way, the visible light photocatalytic activity of H_2O_2 -NTA can be repeatedly renewed.



4. Conclusions

Commercial P25-TiO₂ powder was hydrothermally treated in alkaline medium and pickled to generate NTA with orthorhombic crystal structure. Resultant NTA was then treated in the aqueous solution of H_2O_2 to afford H_2O_2 -NTA photocatalyst possessing apparent visible light photocatalytic activity for the oxidation of propylene. It has been found that H_2O_2 -pretreatment does not alter the band structure but result in the formation of Ti-OOH complexes on the surface of NTA. Surface Ti-OOH complexes serve as visible light absorbing sensitizers to extend photo-response from UV region to visible light region. The higher the Ti-OOH complexes concentration is, the better the visible light absorption is. Under visible light illumination, surface Ti-OOH complexes are excited from the ground state to the excited state, and simultaneously an electron is injected from the excited state to the conduction band of NTA and captured by O_2 to generate $\text{O}_2^{\bullet-}$ radical. It is the highly active $\text{O}_2^{\bullet-}$ radical that accounts for the visible light photocatalytic activity of H_2O_2 -NTA photocatalyst. More importantly, although the visible light photocatalytic activity of photocatalyst H_2O_2 -NTA gradually declines with extending reaction time owing to the consumption of Ti-OOH complexes, it can be renewed by retreatment of the used H_2O_2 -NTA with H_2O_2 . This reminds us that combining metallic semiconductor with metallic-peroxide complexes may help to develop novel photocatalysts with excellent visible light responses and activities. Further investigation in this respect is being underway.

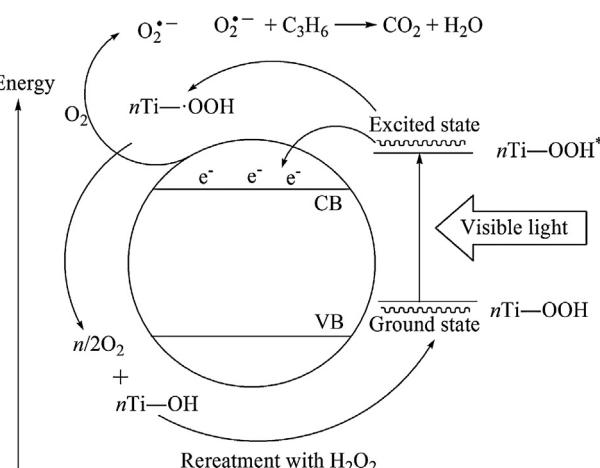
Acknowledgement

We gratefully acknowledge the financial support provided by the National Natural Science Foundation of China (No. 20973054).

References

- [1] T. Kasuga, M. Hiramatsu, A. Hoson, T. Sekino, K. Niihara, *Langmuir* 14 (1998) 3160–3163.
- [2] T. Kasuga, M. Hiramatsu, A. Hoson, T. Sekino, K. Niihara, *Advanced Materials* 11 (1999) 1307–1311.
- [3] S. Yin, S. Uchida, Y. Fujishiro, M. Aki, T. Sato, *Journal of Materials Chemistry* 9 (1999) 1191–1195.
- [4] S. Zhang, J. Zhou, Z. Zhang, Z. Du, A.V. Vorontsov, Z. Jin, *Chinese Science Bulletin* 45 (2000) 1533–1536.
- [5] G. Du, Q. Chen, R. Che, Z. Yuan, L.M. Peng, *Preparation, Applied Physics Letters* 79 (2001) 3702–3704.
- [6] Q. Chen, G. Du, L.M. Peng, *Journal of Chinese Electron Microscopy Society* 21 (2002) 265–269.
- [7] J. Yang, Z. Jin, X. Wang, W. Li, J. Zhang, S. Zhang, X. Guo, Z. Zhang, *Dalton Transactions* 20 (2003) 3898–3901.
- [8] M. Zhang, Z. Jin, J. Zhang, X. Guo, J. Yang, W. Li, X. Wang, Z. Zhang, *Journal of Molecular Catalysis A: Chemical* 217 (2004) 203–210.
- [9] S. Zhang, W. Li, Z. Jin, J. Yang, J. Zhang, Z. Du, Z. Zhang, *Journal of Solid State Chemistry* 177 (2004) 1365–1371.
- [10] L. Qian, Z. Jin, J. Zhang, Y. Huang, Z. Zhang, Z. Du, *Applied Physics A: Materials Science & Processing* 80 (2005) 1801–1805.
- [11] Q. Li, X. Wang, Z. Jin, D. Yang, S. Zhang, X. Guo, J. Yang, Z. Zhang, *Journal of Nanoparticle Research* 9 (2006) 951–957.
- [12] Q. Li, J. Zhang, Z. Jin, D. Yang, X. Wang, J. Yang, Z. Zhang, *Electrochemistry Communications* 8 (2006) 741–746.

Scheme 1. Proposed visible light photocatalytic degradation mechanism of gas propylene over photocatalyst H_2O_2 -NTA.



- [13] J. Yu, H. Yu, B. Cheng, C. Trapalis, *Journal of Molecular Catalysis A: Chemical* 249 (2006) 135–142.
- [14] D.V. Bavykin, S.N. Gordeev, A.V. Moskalenko, A.A. Lapkin, F.C. Walsh, *Journal of Physical Chemistry B* 109 (2005) 8565–8569.
- [15] E. Morgado, B.A. Marinkovic, P.M. Jardin, M.A.S. de Abreu, F.C. Rizzo, *Journal of Solid State Chemistry* 182 (2009) 172–181.
- [16] Z. Jiang, F. Yang, N. Luo, B.T.T. Chu, D. Sun, H. Shi, T. Xiao, P.P. Edwards, *Chemical Communications* (2008) 6372–6374.
- [17] C. Ratanatawanate, Y. Tao, K.J. Balkus Jr., *Journal of Physical Chemistry C* 113 (2009) 10755–10760.
- [18] C. Ratanatawanate, A. Bui, K. Vu, K.J. Balkus, *Journal of Physical Chemistry C* 115 (2011) 6175–6180.
- [19] Q. Zhai, T. Bo, G. Hu, *Journal of Hazardous Materials* 198 (2011) 78–86.
- [20] C. Feng, Y. Wang, Z. Jin, J. Zhang, S. Zhang, Z. Wu, Z. Zhang, *New Journal of Chemistry* 32 (2008) 1038–1047.
- [21] C. Feng, Y. Wang, Z. Jin, S. Zhang, *Acta Physico-Chimica Sinica* 24 (2008) 633–638.
- [22] C. Feng, Z. Jin, J. Zhang, Z. Wu, Z. Zhang, *Photochemistry and Photobiology* 86 (2010) 1222–1229.
- [23] M.A. Khan, H.T. Jung, O.B. Yang, *Journal of Physical Chemistry B* 110 (2006) 6626–6630.
- [24] A. Boonstra, C. Mutsaers, *Journal of Physical Chemistry* 79 (1975) 1940–1943.
- [25] X. Li, C. Chen, J. Zhao, *Langmuir* 17 (2001) 4118–4122.
- [26] T. Ohno, *Journal of Catalysis* 204 (2001) 163–168.
- [27] R. Nakamura, Y. Nakato, *Journal of the American Chemical Society* 126 (2004) 1290–1298.
- [28] Y. Rao, W. Chu, *Environmental Science and Technology* 43 (2009) 6183–6189.
- [29] T. Sano, E. Puzenat, C. Guillard, C. Geantet, S. Matsuzawa, N. Negishi, *Journal of Physical Chemistry C* 113 (2009) 5535–5540.
- [30] Y. Jin, G. Zhao, M. Wu, Y. Lei, M. Li, X. Jin, *Journal of Physical Chemistry C* 115 (2011) 9917–9925.
- [31] Y. Wang, C. Feng, M. Zhang, J. Yang, Z. Zhang, *Applied Catalysis B: Environmental* 104 (2011) 268–274.
- [32] T. Hirakawa, Y. Nosaka, *Langmuir* 18 (2002) 3247–3254.
- [33] T. Hirakawa, K. Yawata, Y. Nosaka, *Applied Catalysis A: General* 325 (2007) 105–111.